

**AQUEOUS ALTERATION AT TYRRHENA TERRA, MARS, AND EVIDENCE FOR GEOTHERMAL PROCESSES.** J. L. Bishop<sup>1</sup>, D. Tirsch<sup>2</sup>, C. E. Viviano<sup>3</sup>, M. D. Lane<sup>4</sup>, L. L. Tornabene<sup>5</sup>, J. R. C. Voigt<sup>6</sup>, F. H. Grant<sup>1,7</sup>, D. Loizeau<sup>8</sup>, L. Sacks<sup>5</sup> and F. Seelos<sup>3</sup>, <sup>1</sup>SETI Institute (Mountain View, CA; jbishop@seti.org), <sup>2</sup>German Aerospace Center (DLR, Berlin, Germany), <sup>3</sup>Johns Hopkins University Applied Physics Lab (Laurel, MD), <sup>4</sup>Fibermetics LLC (Lititz, PA), <sup>5</sup>University of Western Ontario (London, Canada), <sup>6</sup>University of Arizona (Tucson, AZ), <sup>7</sup>UCLA (Los Angeles, CA), and <sup>8</sup>Institut d’Astrophysique Spatiale (CNRS/Univ. Paris-Sud, France).

**Summary:** The central Tyrrhena Terra region features a variety of phyllosilicates and associated alteration minerals including Fe/Mg-smectite, chlorite, serpentine, carbonate, and zeolite. This region is distinct from Libya Montes where Fe/Mg-smectite is the primary phyllosilicate and is commonly associated with olivine. The co-occurrence of chlorite, serpentine, and carbonate or zeolite at the current study site (**Fig. 1**) is consistent with formation through elevated temperatures and is attributed to hydrothermal alteration or diagenesis supported by geothermal flux. We are using coordinated CRISM-TES-THEMIS, CRISM-HRSC-CTX, and CRISM-HiRISE imagery to constrain the presence, stratigraphy, chemistry, and relative ages of olivine, pyroxene, and aqueously altered outcrops.

**Introduction:** A variety of aqueous alteration materials as well as unaltered mafic rocks have been identified through investigations across the region between Isidis and Hellas [e.g. 1-6]. Exposed views of ancient crustal rocks, lava flows from Syrtis Major, alteration from the Isidis and Hellas impact basins, and multiple stream beds and deltas make this region unique on Mars [e.g. 7-10]. Previous studies of morphologic and spectroscopic features using coordinated CRISM-HRSC and CRISM-HiRISE-CTX imagery observed distinct stratigraphic units containing phyllosilicates, carbonate, olivine, and pyroxene at Libya Montes [11-12]. Analyses of geologic features with their associated mineralogy across Tyrrhena Terra revealed differences for the northern border with Isidis, the central region, and the southern area near Hellas [13].

**Orbital Comparison:** We are mapping rock compositions and morphologies using data from multiple spectral and camera imaging systems at Mars including CRISM, TES, THEMIS, HRSC, CTX, and HiRISE. A section of Tyrrhena Terra was selected for this study (**Fig. 1**) based on recent studies of olivine and Fe/Mg-phyllosilicates across Tyrrhena Terra [13-15]. Identification of olivine by TES, THEMIS, and CRISM multispectral data [14] is consistent for most outcrops, and also confirms and extends previous OMEGA detections [16], although different spectral features are used for these instruments.

**Geomorphological Map:** This map of the Tyrrhena Terra region using HRSC nadir image data, CTX imagery, and HRSC DTMs provides a geological and geomorphological overview of the wider region

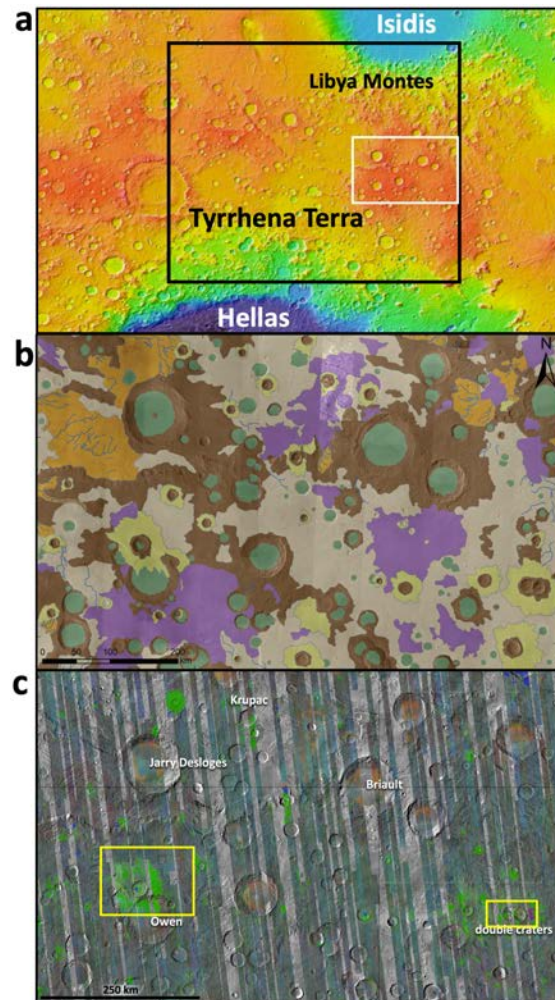


**Fig. 1. A)** Tyrrhena Terra study site marked by white box on MOLA imagery. **B)** geomorphological map [17] over HRSC mosaic highlighting several geologic units including crater floor (cf) materials, ejecta (ej), Noachian/Hesperian massifs (NHm) and fluvially dissected terrains (NHf). **C)** CRISM multispectral mineralogy map [15] with Fe/Mg-phyllosilicates in green, olivine in red, and pyroxene in blue.

and our current study site. The mapping scale was set to 1:500,000 and the HRSC data were down-sampled to a ground pixel size of 50 m/px for image data and 100 m/px for the DTMs, respectively [17].

**CRISM Views:** We evaluated spectra from targeted CRISM images at two sites offering good coverage of phyllosilicates and associated alteration materials (**Fig. 1C**). We employed the MTRDR calibration [18] of these

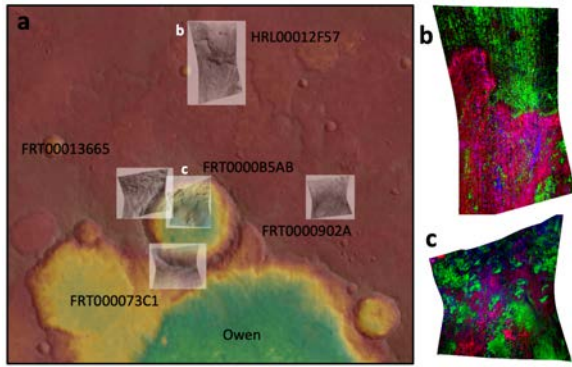


**Fig. 2. A)** HRSC view with CRISM IRB images on top. False color mineralogy viewed in CRISM images **B)** HRL00012F57 and **C)** FRT0000B5AB with  $R=D2300$ ,  $G=BDI2000$ ,  $B=BD1900\_2$  featuring pyroxene in green, chlorite in red, chlorite/smectite in pink, Fe/Mg-smectite in purple, and additional hydrated phases in blue.

images and tested several parameter combinations [19] to highlight variations in mafics, Fe/Mg-phyllsilicates, and associated aqueous outcrops across these scenes. Image FRT0000B5AB exposes pyroxene and Mg-rich phyllsilicates in a small crater north of Owen crater and image HRL00012F57 is associated with fluvial features that have eroded phyllsilicate-rich ejecta north of this crater (**Fig. 2A**). These CRISM images highlight variations in phyllsilicate type with Fe/Mg-smectite (mostly saponite) mapped in purple and Mg-rich phyllsilicates (mostly chlorite) mapped in red (**Figs. 2B&C**). Hydrated phases in image HRL00012F57 are mapped in blue that are consistent with zeolite and the small, bright red outcrop at the central mound in image FRT0000B5AB includes carbonate similar to dolomite. Spectra of these outcrops are shown in **Fig. 3**. Images HRL00013F70 and HRL0000119C7 occur at the double crater site in the SE part of our study site (**Fig. 4A**). Blocky outcrops of chlorite-smectite, Fe/Mg-smectite, and hydrated materials (including zeolites) occur in

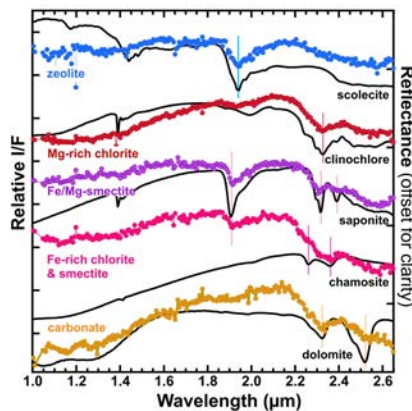


**Fig. 3.** Selected ratioed CRISM spectra of chlorite, chlorite/smectite, smectite, zeolite, and carbonate from our study site compared to lab spectra of minerals.

these images around the crater walls, while smaller mixed outcrops of chlorite and chlorite-smectite are detected in the central mounds (**Figs. 4B&C**); spectra are shown in **Fig. 3**.

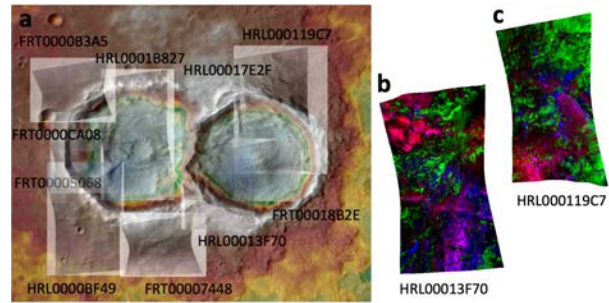


**Fig. 4. A)** HRSC view with CRISM IRB images overlain. **B)** HRL00013F70 and **C)** HRL0000119C7 with the same parameters as Fig. 2.

**Implications for Aqueous Alteration and Geologic Processes:** Fe/Mg-phyllsilicates are the dominant aqueous mineral across the Tyrrhena Terra region and are more abundant in the central region compared to regions near Isidis or Hellas [15]. High temperature phyllsilicates including chlorite, serpentine, and prehnite increase in abundance with distance from both impact basins [13,15]. The current study site, where increased abundances of high-temperature phyllsilicates, zeolite and carbonate are observed, is associated with a region of elevated groundwater from geothermal flux where hydrothermal activity is proposed [20]. Thus, the alteration materials investigated here at the central Tyrrhena Terra region may have been produced via hydrothermal alteration and diagenesis of previously formed Fe/Mg-smectites. These smectites appear to be widespread from Libya Montes through the central Tyrrhena Terra region. Sparsely distributed, tiny carbonate outcrops are observed both at Libya Montes [11] and central Tyrrhena Terra that could have resulted from localized hydrothermal activity; however, the substantial chlorite observed in the current study, together with zeolite is consistent with highly advanced hydrothermal alteration.

**Acknowledgements:** We are grateful for support from MDAP grant # 80NSSC18K1384.

**References:** [1] Craddock R. (1994) *LPSC*, 291-292. [2] Ivanov M. & Head J. (2003) *JGR*, 108, E6. [3] Rogers A. & Christensen P. (2007) *JGR*, 112, E01003. [4] Tornabene L. et al. (2008) *JGR*, 113, E10001. [5] Loizeau D. et al. (2012) *Icarus*, 219, 476-497. [6] Rogers A. & Hamilton V. (2015) *JGR*, 120, 62-91. [7] Crumpler L. & Tanaka K. (2003) *JGR*, 108, 12. [8] Jaumann R. et al. (2010) *EPSL*, 294, 272-290. [9] Erkeling G. et al. (2012) *Icarus*, 219, 393-413. [10] Ivanov, M. et al. (2012) *Icarus*, 218, 24-46. [11] Bishop J. et al. (2013) *JGR*, 118, 487-513. [12] Tirsch D. et al. (2018) *Icarus*, 314, 12-34. [13] Tirsch D. et al. (2021) *LPSC*, #1193. [14] Lane M. et al. (2021) *LPSC*, #2550. [15] Viviano C. & M. Phillips (2019) *9th Mars Conf.*, #6359. [16] Ody A. et al. (2013) *JGR*, 118, 234-262. [17] Tirsch D. et al. (2019) *LPSC*, #1532. [18] Seelos F. et al. (2016) *LPSC*, #1783. [19] Viviano-Beck C. et al. (2014) *JGR*, 119, 2014JE004627. [20] Ojha L. et al. (2020) *Sci. Adv.*, 6 (49), eabb1669.